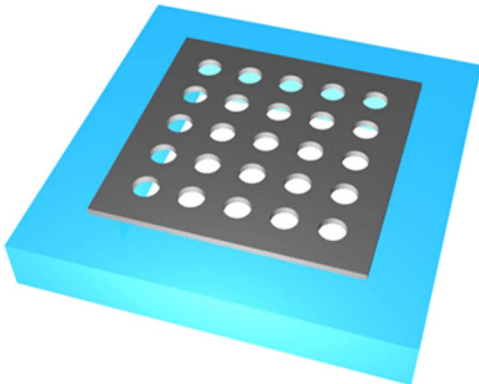


# Fano-Resonance Photonic Crystal Membrane Reflectors at Mid- and Far-Infrared

Volume 5, Number 1, February 2013

Yichen Shuai  
Deyin Zhao  
Gautam Medhi  
Robert Peale  
Zhenqiang Ma, Member, IEEE  
Walter Buchwald  
Richard Soref, Fellow, IEEE  
Weidong Zhou, Senior Member, IEEE



---

DOI: 10.1109/JPHOT.2013.2240446  
1943-0655/\$31.00 ©2013 IEEE

# Fano-Resonance Photonic Crystal Membrane Reflectors at Mid- and Far-Infrared

**Yichen Shuai,<sup>1</sup> Deyin Zhao,<sup>1</sup> Gautam Medhi,<sup>2</sup> Robert Peale,<sup>2</sup> Zhenqiang Ma,<sup>3</sup> Member, IEEE, Walter Buchwald,<sup>4</sup> Richard Soref,<sup>4</sup> Fellow, IEEE, and Weidong Zhou,<sup>1</sup> Senior Member, IEEE**

<sup>1</sup>Department of Electrical Engineering, NanoFAB CenterUniversity of Texas at Arlington, TX 76019 USA  
<sup>2</sup>Physics Department, University of Central Florida, Orlando, FL 32816 USA

<sup>3</sup>Department of Electrical and Computer Engineering, University of WI-Madison, WI 53706 USA

<sup>4</sup>Department of Physics and Engineering Program, University of Massachusetts, Boston, MA 02125 USA

DOI: 10.1109/JPHOT.2013.2240446  
1943-0655/\$31.00 ©2013 IEEE

Manuscript received December 14, 2012; accepted January 12, 2013. Date of publication January 16, 2013; date of current version February 4, 2013. This work was supported in part by U.S. ARO under Grant W911NF-09-1-0505 and in part by AFOSR MURI Program FA9550-08-1-0337. Corresponding author: W. Zhou (e-mail: wzhou@uta.edu).

**Abstract:** We report here single-layer ultracompact Fano-resonance photonic crystal membrane reflectors (MRs) at mid-infrared (IR) and far-IR (FIR) bands, based on single layer crystalline Si membranes. High-performance reflectors were designed for surface-normal incidence illumination with center operation wavelengths up to the  $75\text{-}\mu\text{m}$  FIR spectral band. Large-area patterned MRs were also fabricated and transferred onto glass substrates based on membrane transfer processes. Close to 100% reflection was obtained at the  $\sim 76\text{-}\mu\text{m}$  spectral band, with a single-layer Si membrane thickness of  $18\text{ }\mu\text{m}$ . Such Fano-resonance-based membranes reflectors offer great opportunities for high-performance ultracompact dielectric reflectors at IR and THz regions.

**Index Terms:** Fano resonance, photonic crystals, membrane reflectors, infrared photonics, silicon photonics.

## 1. Introduction

Compact broadband reflectors are of great importance for optoelectronic devices and photonic integrated circuits like lasers, photodetectors, solar cells, and sensors. Traditionally, they can be realized by using metal or stacked dielectric thin films. Metal films offer larger reflection bandwidth but are limited by their intrinsic absorption losses. Stacked dielectric distributed Bragg reflectors (DBRs) can achieve very low losses, but they typically require many individual layers with stringent refractive index and thickness tolerances for each layer. It becomes a difficult engineering challenge to realize extremely high-reflection DBRs at mid-infrared (IR) and far-IR (FIR), and THz frequencies, due to the scaling of the dielectric quarter-wavelength stack.

Recently, broadband reflectors based on Fano resonance or guided mode resonance [1]–[5] have attracted great attention, where high reflectivity can be obtained with a single-layer 1-D high-contrast grating (HCG) [6] or a 2-D photonic crystal slab (PCS) structure [5]. By properly controlling the design parameters, very broadband reflectors can be obtained. Based on crystalline membrane transfer, high-performance membrane reflectors (MRs) and lasers at near-IR (NIR; 1550nm) have been reported recently fabricated on crystalline Si, SOI and on glass substrates [5], [7], [8].

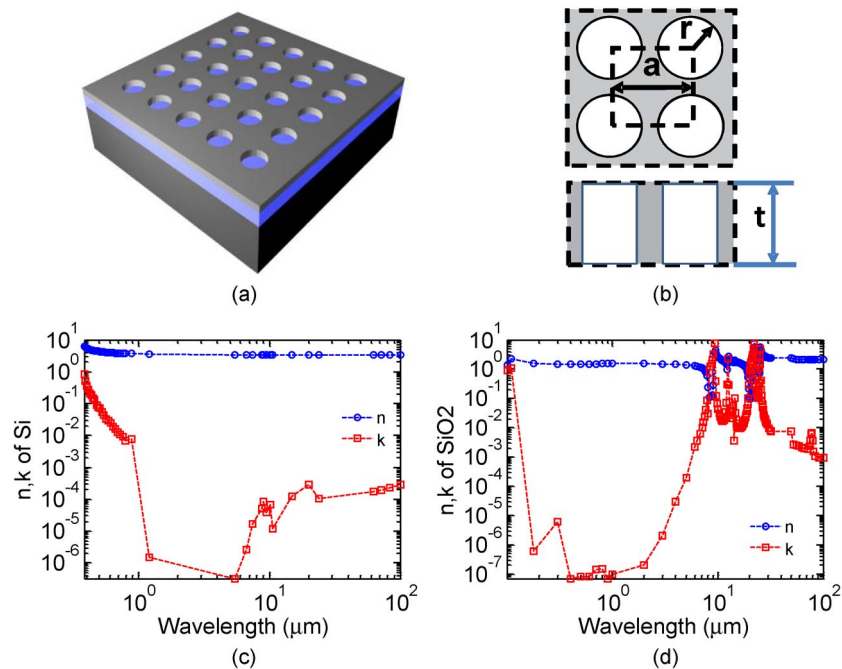


Fig. 1. (a) 3-D sketch of a Si MR with a patterned 2-D air hole square lattice photonic crystal structure on SOI substrate; (b) Key lattice parameters for the square lattice air hole photonic crystal structures are air hole radius ( $r$ ), lattice constant (period  $a$ ), and Si-MR thickness ( $t$ ); (c) and (d), Complex index parameters for Si and  $\text{SiO}_2$  used in the simulation.

We report here single-layer ultracompact Si-MRs at mid-IR and FIR bands, based on a suspended membrane structure. High-performance reflectors were designed for surface-normal incidence with center operation wavelengths of 1.5  $\mu\text{m}$ , ~9  $\mu\text{m}$ , 32  $\mu\text{m}$ , and 75  $\mu\text{m}$ , respectively. Large-area patterned MRs were also fabricated and transferred onto glass substrates using a PDMS-stamp-assisted membrane transfer printing process. Close to 100% reflectivity was obtained at the ~76  $\mu\text{m}$  spectral band, with a single-layer Si membrane thickness of 18  $\mu\text{m}$ .

## 2. MR Design

As shown schematically in Fig. 1(a), a square lattice air hole photonic crystal structures on SOI substrate is used for our design. The key lattice parameters are shown in Fig. 1(b), where  $r$ ,  $a$ , and  $t$  represent air hole radius, lattice constant (period), and Si-MR thickness, respectively. The complex index parameters for Si and  $\text{SiO}_2$  used in the design are shown in Fig. 1(c) and Fig. 1(d), respectively [9]. The chosen design parameters were based on finite-difference time-domain (FDTD) simulations and rigorous coupled-wave analysis (RCWA) techniques [10]. Shown in Fig. 2 are the simulated reflector performances for designs at four different wavelength bands. All designs are based on suspended (in air) Si-MR configurations. Broadband reflection with 100% peak reflection is achieved for all designed wavelength bands, with the optimal selection of lattice parameters and Si thicknesses. Based on scaling principles, it was found that the optimal Si-MR thickness ( $t$ ) is  $\sim 0.75 - 0.85$  ( $\lambda/n$ ), and the optimal lattice constant ( $a$ ) is  $\sim 1.9 - 2.1$  ( $\lambda/n$ ), where  $\lambda$  is the wavelength and  $n$  is the refractive index of Si.

## 3. MR Fabrication

The Si-MR fabrication process flow is shown schematically in Fig. 3. Patterns were first formed in photoresist on SOI substrates using either e-beam lithography or optical lithography, depending on the feature size required for the different spectral bands. This was followed by a reactive-ion etching (RIE) process to transfer the pattern into the host material. The patterned Si membrane structures

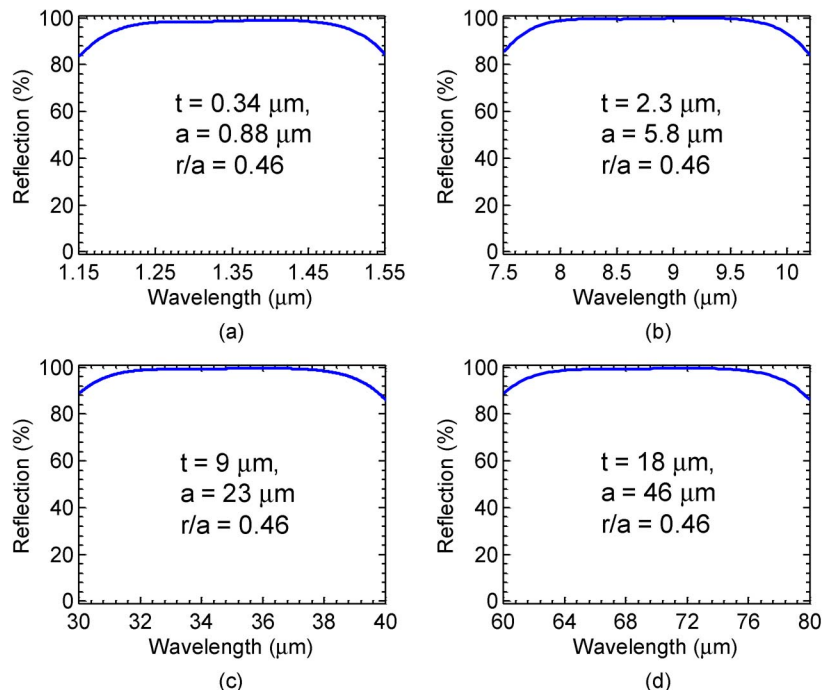


Fig. 2. Simulated reflector performances for designs at four different wavelength bands.

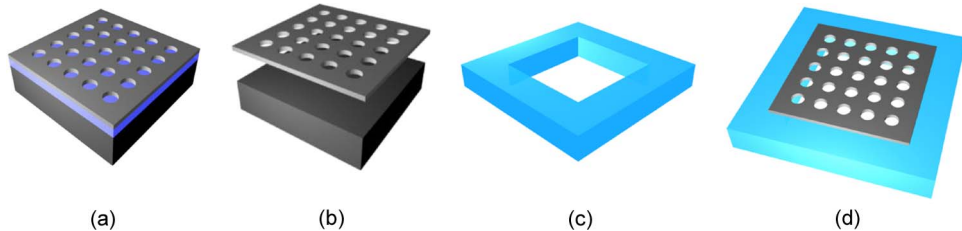


Fig. 3. Si-MR schematic fabrication process flow: (a) Photonic crystal structure patterned on SOI substrate; (b) Release of patterned top Si-MR layer from Si substrate by selective wet-etching; (c) Preparation of host substrates with center openings; and (d) Final suspended Si-MR on host substrate.

were then released by a selective buffered oxide etchant (BOE) etching of the buried oxide (BOX) layer. Finally, the patterned single-layer Si membrane was transferred onto a transparent foreign substrate, such as glass. In order to avoid the strong absorptions in the  $\text{SiO}_2$  material for wavelengths greater than  $5 \mu\text{m}$  [see Fig. 1(d)], an open hole was formed on the transparent glass substrate to produce a suspended Si-MR [11].

Shown in Fig. 4 are images of the fabricated Si-MR at the  $76\text{-}\mu\text{m}$  spectral band patterned using optical lithography. As shown in Fig. 4(a), up to a  $1''$  square high-quality patterned area was formed, with excellent uniformity [see Fig. 4(b)]. The structure was released and transferred onto a piece of glass substrate to form a suspended membrane Si-MR, as shown in Fig. 4(c).

#### 4. MR Characterization

Various measurement setups have been used for Si-MR reflection measurements in different spectral regions. For NIR structures, a free-space beam splitter was used for surface-normal reflection measurement, with a gold reflector used as reference [12]. For longer wavelengths (MWIR to LWIR), a Nicolet micro-Fourier transform IR (FTIR) system was used, where the reflection measurement was

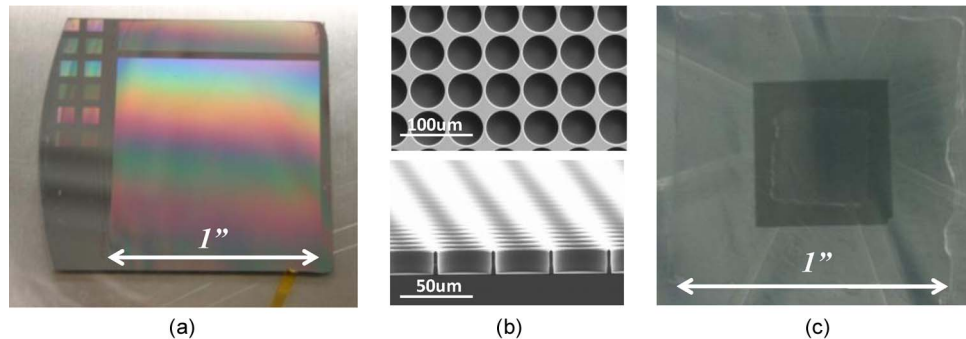


Fig. 4. (a) A micrograph of a fabricated Si-MR on SOI; (b) Scanning-electron micrographs (SEMs) of a fabricated Si-MR at the  $76\text{ }\mu\text{m}$  spectral band, top and 3-D views; and (c) a micrograph of a transferred Si-MR at the  $76\text{ }\mu\text{m}$  spectral band on a glass substrate with a center opening to form a suspended Si-MR.

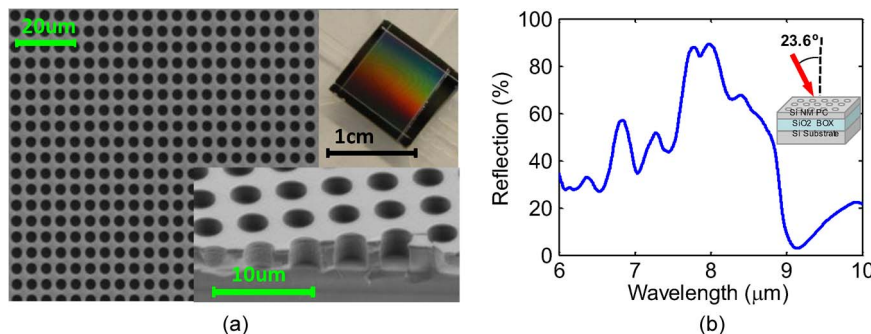


Fig. 5. (a) A SEM top-view image of the fabricated Si-MR at mid-IR, with a cross-sectional SEM image and a micrograph shown in the insets; (b) Measured reflection spectrum for a Si-MR on  $4\text{ }\mu\text{m}$   $\text{SiO}_2$  box layer measured at an incident angle of  $23.6^\circ$  off surface-normal measured with a micro-FTIR system.

carried out with a  $23.6^\circ$  off-surface-normal beam, through a  $15\times 0.4\text{NA}$  reflecting objective lens. A SEM top-view image of the fabricated Si-MR at  $8\text{-}\mu\text{m}$  spectral band is shown in Fig. 5(a), along with a cross-sectional SEM image and a micrograph shown in the insets. High-quality uniform pattern with size  $\sim 1\text{ cm}^2$  area was achieved. Measured reflection spectrum is shown in Fig. 5(b), where the measured was carried out with a  $23.6^\circ$  off-surface-normal beam. Close to 90% peak reflection was achieved. It is worth notice that these MRs are very sensitive to incident angles. It is anticipated that the surface-normal reflection for this MR can be much higher.

To estimate the reflectivity of the Fano reflector at FIR, a Fabry–Perot interferometer was formed from two identical reflectors and its finesse characterized. The finesse  $F$  may be determined from the free spectral range (FSR;  $\Delta\lambda$ ) and the resonance full width at half-maximum (FWHM;  $\delta\lambda$ ) according to  $F = \Delta\lambda/\delta\lambda$ . The reflectivity  $R$  is then found from the measured finesse according to  $F = \pi\sqrt{R/(1-R)}$  [13].

The FIR measurement setup is shown in Fig. 6(a). One of the Fano reflectors was mounted on a fixed mirror mount. The second was mounted on a computer-controlled motorized precision translational stage. Radiation from a quantum cascade laser (QCL) at  $70\text{-}\mu\text{m}$  wavelength was collimated by a  $90^\circ$  off-axis parabolic mirror and passed through the Fabry–Perot cavity, where it was focused onto a slow but sensitive Golay cell detector by a second off-axis paraboloid. The QCL (Trion) was held at  $77\text{ K}$  inside a liquid nitrogen cryostat with a polyethylene output window. The collimating optic was inside the cryostat. The laser was excited with a burst of fifty  $10\text{-}\mu\text{s}$ -long pulses. The repetition rate of the burst was  $\sim 10\text{ Hz}$ , and the burst duty cycle was 50%. The optical transmission

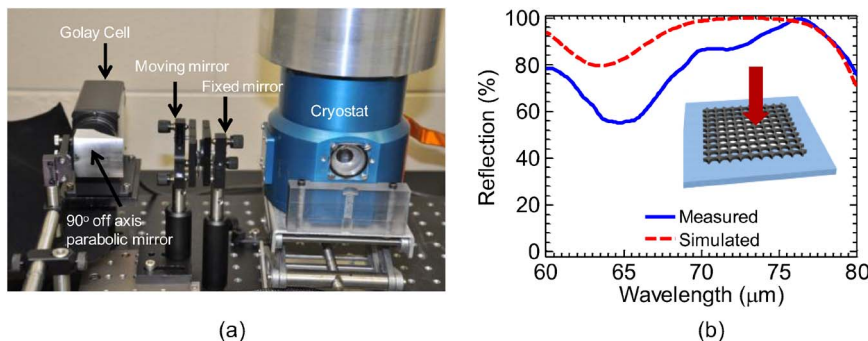


Fig. 6. (a) A photograph of the experimental setup for the measurement of Si-MR reflection at the  $76\text{ }\mu\text{m}$  spectral band; (b) Measured and simulated reflection spectra for a suspended Si-MR on glass.

spectrum, integrated by the Golay cell and lock-in amplified at the slow burst repetition rate, was recorded.

Shown in Fig. 6(b) are the measured and simulated surface-normal reflection spectrum outputs derived from transmission measurements. Assuming no absorption in the spectral band, we can obtain close to 100% reflection at roughly  $76\text{-}\mu\text{m}$  wavelength. The experimental results agree reasonably well with the simulation results.

## 5. Conclusion

We have performed detailed design studies, experimental fabrication, and IR measurements on ultracompact single-layer silicon photonic-crystal Fano MRs for the mid-IR and FIR spectral regions. We have attained very high reflectivity (approaching 100%) over a broad spectral band with this all-dielectric semiconductor membrane and the observed results agreed well with simulations. High-reflectivity Si membranes have been obtained at the IR center wavelengths of  $8\text{ }\mu\text{m}$  and  $76\text{ }\mu\text{m}$ . The results here indicate that a variety of high-Q membrane-cavity enhanced applications will be feasible in chem–bio sensors, lasers, photodetectors, photovoltaics, and filters; uses that would, in many cases, employ a Fabry–Perot resonator comprised of two parallel membranes, yielding a Q-factor higher than that provided by competing techniques.

## Acknowledgment

The authors appreciate guidance and help from Dr. M. Gerhold and Dr. G. Pomrenke.

## References

- [1] M. C. Y. Huang, Y. Zhou, and C. J. Chang-Hasnain, “A surface-emitting laser incorporating a high-index-contrast subwavelength grating,” *Nat. Photon.*, vol. 1, no. 2, pp. 119–122, Feb. 2007.
- [2] S. Boutami, B. Bakir, P. Regreny, J. Leclercq, and P. Viktorovitch, “Compact  $1.55\text{ }\mu\text{m}$  room-temperature optically pumped VCSEL using photonic crystal mirror,” *Electron. Lett.*, vol. 43, no. 5, pp. 37–38, Mar. 2007.
- [3] R. Magnusson and S. S. Wang, “New principle for optical filters,” *Appl. Phys. Lett.*, vol. 61, no. 9, pp. 1022–1024, Aug. 1992.
- [4] S. Fan and J. D. Joannopoulos, “Analysis of guided resonances in photonic crystal slabs,” *Phys. Rev. B*, vol. 65, pp. 235112-1–235112-8, 2002.
- [5] H. Yang, D. Zhao, S. Chuwongin, J. H. Seo, W. Yang, Y. Shuai, J. Berggren, M. Hammar, Z. Ma, and W. Zhou, “Transfer-printed stacked nanomembrane lasers on silicon,” *Nat. Photon.*, vol. 6, no. 9, pp. 617–622, Sep. 2012.
- [6] C. J. Chang-Hasnain, “High-contrast gratings as a new platform for integrated optoelectronics,” *Semicond. Sci. Technol.*, vol. 26, no. 1, p. 014043, Jan. 2011.
- [7] W. Zhou, Z. Ma, H. Yang, Z. Qiang, G. Qin, H. Pang, L. Chen, W. Yang, S. Chuwongin, and D. Zhao, “Flexible photonic-crystal Fano filters based on transferred semiconductor nanomembranes,” *J. Phys. D, Appl. Phys.*, vol. 42, no. 23, pp. 234 007–234 017, Dec. 2009.
- [8] Z. Qiang, H. Yang, S. Chuwongin, D. Zhao, Z. Ma, and W. Zhou, “Design of Fano broadband reflectors on SOI,” *IEEE Photon. Technol. Lett.*, vol. 22, no. 15, pp. 1108–1110, Aug. 2010.
- [9] E. D. Palik, *Handbook of Optical Constants of Solids*, vol. 1, New York, NY, USA: Academic, 1985.

- [10] D. Zhao, H. Yang, S. Chuwongin, J. H. Seo, Z. Ma, and W. Zhou, "Design of photonic crystal membrane reflector based VCSELs," *IEEE Photon. J.*, vol. 4, no. 6, pp. 2169–2175, Dec. 2012.
- [11] H. C. Yuan and Z. Ma, "Microwave thin-film transistors using Si nanomembranes on flexible polymer substrate," *Appl. Phys. Lett.*, vol. 89, no. 21, pp. 212105-1–212105-3, Nov. 2006.
- [12] H. Yang, D. Zhao, J. Seo, S. Kim, J. Rogers, Z. Ma, and W. Zhou, "Broadband membrane reflectors on glass," *IEEE Photon. Technol. Lett.*, vol. 24, no. 6, pp. 476–478, Mar. 2012.
- [13] B. E. A. Saleh, M. C. Teich, and B. E. Saleh, *Fundamentals of Photonics*. New York, USA: Wiley, 1991.